Research Article

Magnetic Resonance in Chemistry

Received: 19 July 2012 Revised: 12 September 2012 Accepted: 11 December 2012 Published online in Wiley Online Library: 10 January 2013

(wileyonlinelibrary.com) DOI 10.1002/mrc.3919

Synthesis and characterization of an MRI Gd-based probe designed to target the translocator protein

Erika Cerutti,[a] Annelaure Damont,[b] Frédéric Dollé,[b] Simona Baroni[c] and Silvio Aime[a]*

DPA-713 is the lead compound of a recently reported pyrazolo[1,5-a]pyrimidineacetamide series, targeting the translocator protein (TSPO 18 kDa), and as such, this structure, as well as closely related derivatives, have been already successfully used as positron emission tomography radioligands. On the basis of the pharmacological core of this ligands series, a new magnetic resonance imaging probe, coded DPA-C_6-(Gd)DOTAMA was designed and successfully synthesized in six steps and 13% overall yield from DPA-713. The Gd-DOTA monoamide cage (DOTA = 1,4,7,10-tetraazacyclododecane-1,4,7,10-tetraacetic acid) represents the magnetic resonance imaging reporter, which is spaced from the phenylpyrazolo[1,5-a]pyrimidineacetamide moiety (DPA-713 motif) by a six carbon-atom chain. DPA-C_6-(Gd)DOTAMA relaxometric characterization showed the typical behavior of a small-sized molecule (relaxivity value: 6.02 $mM^{-1} s^{-1}$ at 20 MHz). The good hydrophilicity of the metal chelate makes DPA-C_6-(Gd)DOTAMA soluble in water, affecting thus its biodistribution with respect to the parent lipophilic DPA-713 molecule. For this reason, it was deemed of interest to load the probe to a large carrier in order to increase its residence lifetime in blood. Whereas DPA-C_6-(Gd)DOTAMA binds to serum albumin with a low affinity constant, it can be entrapped into liposomes (both in the membrane and in the inner aqueous cavity). The stability of the supramolecular adduct formed by the Gd-complex and liposomes was assessed by a competition test with albumin. Copyright © 2013 John Wiley & Sons, Ltd.

Keywords: NMR; ^{1}H; MRI; contrast agents; relaxometry; Gd-complexes; DPA-713; TSPO

Introduction

The translocator protein (TSPO-18 kDa), formerly known as peripheral benzodiazepine receptor,[1] is a five-transmembrane protein[2] localized primarily on the outer mitochondrial membrane.[1,3] TSPO is expressed in many organs, but it is expressed at the highest level in steroidogenic cells, where TSPO is involved in the translocation of cholesterol from the outer to the inner mitochondrial membranes. TSPO is also located in the central nervous system where it is usually expressed in microglia[4,5] and in some neuronal cell types.[6–9] Following neuronal injury, TSPO expression is dramatically increased, in particular, in the case of Alzheimer disease and multiple sclerosis.[10,11] Microglia are extremely sensitive toward alterations due to neuronal injury. Until now, positron emission tomography has been the most used medical imaging technique in the study of how microglia are involved in degenerative diseases. Different TSPO targeting molecules have been synthesized over the past two decades. They belong to different chemical classes,[12–14] but the most promising one is the 2-phenylpyrazolo[1,5-a]pyrimidineacetamide series[15,16], which includes, among others, the two following radiotracers: [^{11}C]DPA-713[17–19] and [^{18}F]DPA-714.[20–25,27,28]

Magnetic resonance imaging (MRI) is a non-invasive technique that allows morphology, physiology and metabolism visualization *in vivo*. MRI images deal with water ^{1}H proton spatial localization, whose intensity is sufficiently high, thanks to the high concentration of water in living organisms. The main advantage of this technique is its superb spatial resolution (in ordinary image acquisition, a resolution of 100 μm is attained), but its major drawback is represented by the low sensitivity of its probes.[28]

A novel MRI Gd-based probe has therefore been designed, combining the pharmacological properties of the DPA-713 core with a gadolinium-dedicated (DOTA) chelator. The conjugation site was selected on the basis of previous SAR studies having shown that chemical flexibility was permitted at the para position of the phenyl ring.[29] A spacer of six carbon atoms was moreover introduced to minimize the steric hindrance of the DOTA cage at the interaction site of the molecule with TSPO. As the development of an MRI targeting agent requires systems that remain in circulation for a long time, the interaction of DPA-C_6-(Gd)DOTAMA with human serum albumin (HSA) and its incorporation into liposomes have been explored. Moreover, the latter systems can act as carriers for a great number of imaging reporter units thus offering a route to overcome the sensitivity issue associated to MR applications.

* *Correspondence to: Silvio Aime, Dipartimento di Chimica and Centro di Imaging Molecolare, Università degli Studi di Torino, V. Nizza 52, 10126 Torino, Italy. E-mail: silvio.aime@unito.it*

a *Dipartimento di Chimica and Centro di Imaging Molecolare, Università degli Studi di Torino, Via Nizza 52, 10126, Torino, Italy*

b *CEA, I^{2}BM, Service Hospitalier Frédéric Joliot, 4 Place du Général Leclerc, F-91406, Orsay, France*

c *Invento Srl, Via Nizza 52, Torino, Italy*

Results and Discussion

DPA-C_6-(Gd)DOTAMA (**1**) was synthesized in six steps from DPA-713 and obtained in 13% overall and non-optimized yield (Scheme 1). Briefly, DPA-713, as starting material, was synthesized according to literature procedures.[17] *O*-demethylation of DPA-713 was carried out with a 1 M solution of BBr_3 in dichloromethane at low temperature (from −60 to −20 °C) affording the corresponding phenol **2** (DPA-OH) in high yield (95%).[20] The aminohexyl spacer was introduced into the structure by coupling the DPA-skeleton **2** with 6-(Boc-amino)hexan-1-ol activated as a sulfonate (synthesized as described in the experimental part) in DMSO at 50 °C in the presence of NaOH as a base, to afford product **3** in moderate yield (63%). The Boc protecting group was removed using trifluoroacetic acid in dichloromethane, giving the free amine (**4**) in 80% yield. Coupling of **4** with DOTA$(tBu)_3$[30] was carried out in the presence of TBTU and DIPEA in DMF yielding the DOTAMA derivative **5** in 80% yield. *Tert*-Butyl groups were then removed using trifluoroacetic acid to afford **6** (DPA-C_6-DOTAMA) in 33% yield after chromatography purification. The ligand complexation was carried out by stoichiometric addition of $GdCl_3$ maintaining the pH at 6.5 by addition of a 0.1 N aqueous NaOH solution.

Relaxometric characterization of DPA-C_6-(Gd)DOTAMA (1)

The relaxivity of **1** (i.e. the change of the water proton relaxation rate in the presence of the paramagnetic complex at 1 mM concentration) measured at 20 MHz and 20 °C was 6.02 $mM^{-1}\,s^{-1}$. This value was slightly higher than that reported in literature[31] for the parent Gd-DOTAMA complex (r_{1p} = 4.7 $mM^{-1}\,s^{-1}$). The nuclear magnetic resonance dispersion (NMRD) profile was also acquired (Figure 1) and found to show the typical behavior of small gadolinium complexes.

The NMRD data were fitted to the values calculated on the basis of the established paramagnetic relaxation theory,[32] and the obtained values are reported in Table 1 together with the corresponding ones of the parent Gd-DOTAMA-C_6-OH. Going from Gd-DOTAMA-C_6-OH to **1**, the increased molecular weight

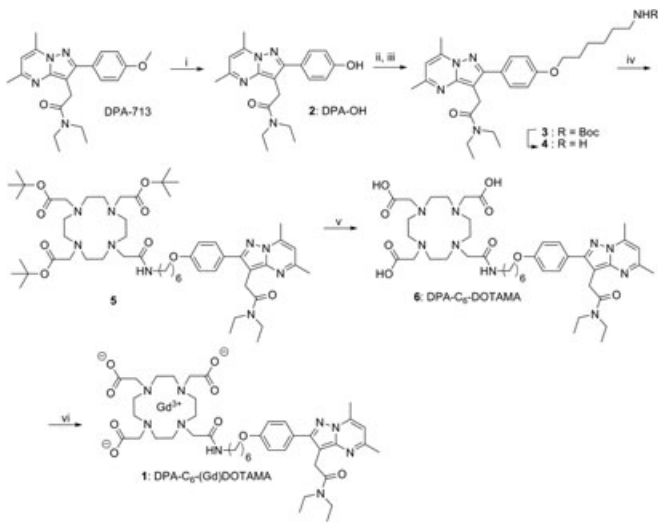

Scheme 1. Synthesis of DPA-C_6-(Gd)DOTAMA. (i) BBr_3, CH_2Cl_2 anhydr., −60 °C to −20 °C, 5 h; (ii) 6-((*tert*-butoxycarbonyl) amino)hexyl 4-methylbenzenesulfonate, NaOH, DMSO, 50 °C, overnight; (iii) TFA, CH_2Cl_2, RT, 24 h; (iv) DOTA$(tBu)_3$, TBTU, DIPEA, DMF, RT, 24 h; (v) TFA, CH_2Cl_2, RT, 24 h; (vi) $GdCl_3 \times 6H_2O$, pH = 6.5, RT.

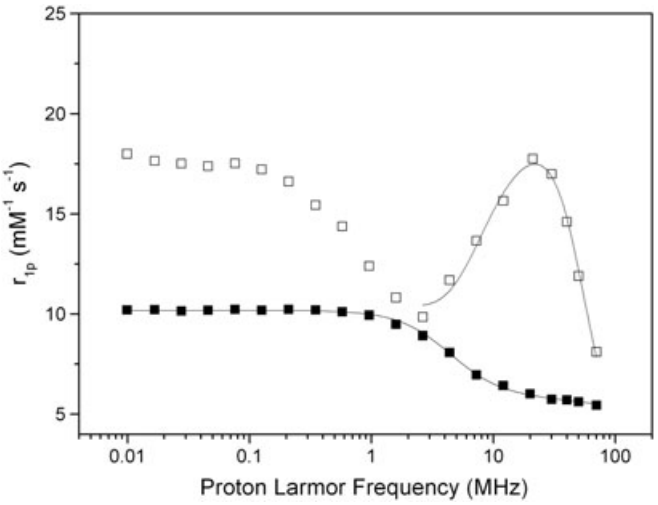

Figure 1. $1/T_1$ nuclear magnetic resonance dispersion profile of 1 mM aqueous solution of DPA-C_6-(Gd)DOTAMA (■) and human serum albumin adduct (□) at 25 °C and pH = 7.4.

Table 1. Best fitting parameters for from the analysis of the nuclear magnetic resonance dispersion profile of **1**

	Δ^2 ($10^{19}\,s^{-2}$)	τ_v (ps)	τ_r (ps)	τ_m (μs)	q	r_{1p} ($mM^{-1}\,s^{-1}$)[a]
DPA-C_6-(Gd)DOTAMA (**1**)	2.65	27	114	1.4	1	6.02
Gd-DOTAMA-C_6-OH	1.4	40	70	1.3	1	4.7

[a]Measured at 25 °C at 20 MHz.

is responsible for the markedly longer molecular re-orientational time τ_r, which in turn is the main determinant of the increase of the observed relaxivity.

Interaction of DPA-C_6-(Gd)DOTAMA (1) with HSA

Human serum albumin is the most abundant protein in blood and often acts as carrier for metabolites, nutrients and drugs. The lipophilicity of the DPA-713 moiety anticipates the possible binding of **1** to HSA. Binding parameters (the affinity constant K_A and the relaxivity of supramolecular adduct r_{1p}^{bound}) were determined using the proton relaxation enhancement (PRE) method.[33] The experimental procedure consists of carrying out a titration in which a fixed quantity of Gd-complex (0.19 mM) is titrated with increasing concentrations of the macromolecular host (Figure 2). The observed relaxation rates increase according to K_A and r_1^{bound} values. In this case, a K_A of 1100 M^{-1} and an r_1^{bound} of 20 $mM^{-1}\,s^{-1}$ were determined.

The obtained K_A value demonstrates that there is a relatively weak interaction between **1** and albumin. The calculated r_1^{bound} is markedly higher than the r_{1p} of the free DPA-C_6-(Gd)DOTAMA (**1**), in accordance with the formation of the adduct with albumin that is characterized by a markedly slower tumbling rate.

The NMRD profile of a solution containing DPA-C_6-(Gd) DOTAMA (**1**) and HSA in ca. 1:1 ratio (0.19 mM of **1** and 0.2 mM of HSA) was acquired (data not shown). On the basis of the previously mentioned reported results, compound **1** is only in part bound to HSA. From the knowledge of the affinity constant (K_A) and the millimolar relaxivity of the bound fraction (r_1^{bound}), it

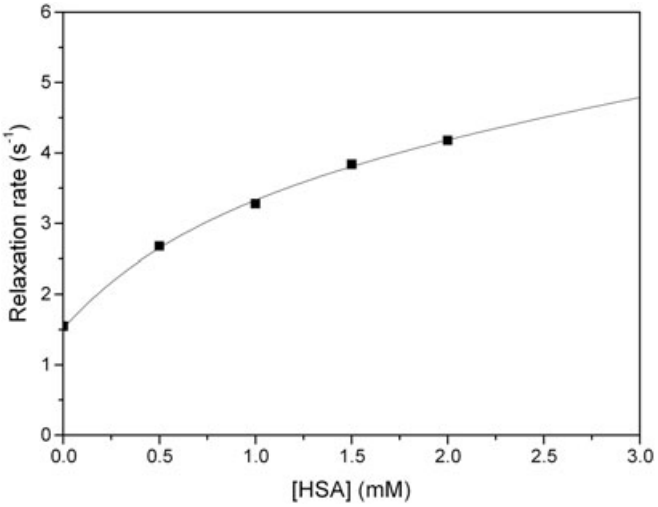

Figure 2. Determination of binding association constants K_A between DPA-C_6-(Gd)DOTAMA (**1**) and human serum albumin at 25 °C and pH = 7.4.

has been possible to quantify as 68% the percentage of compound **1** bound to HSA under the applied 1:1 ratio. From these data, the NMRD profile for the fraction of DPA-C_6-(Gd)DOTAMA bound to HSA has been calculated (Figure 1), and the high field relaxivity values fitted according to the theory of paramagnetic relaxation enhancement. The values obtained for the relevant parameters are reported in Table 2.

On going from the free complex (**1**) to the adduct with HSA, a high relaxivity peak centered at ca. 40 MHz is observed for the latter species indicative of a relaxivity domain determined by the molecular re-orientational time (τ_r). In fact, from the NMRD analysis, τ_r is markedly increased if compared with free DPA-C_6-(Gd)DOTAMA, as expected. The relaxivity obtained at 20 MHz for the macromolecular adduct with HSA is 17.5 $mM^{-1}\,s^{-1}$, i.e. almost three times larger than the value obtained for free DPA-C_6-(Gd)DOTAMA.

Entrapment of DPA-C_6-(Gd)DOTAMA (1) in liposomes

Entrapment into liposomes of DPA-C_6-(Gd)DOTAMA (**1**) has been taken into account to increase the circulation lifetime and to pursue a slow release of the compound of interest. Two types of liposome have been prepared, namely LP1 and LP2. Both liposomes were prepared by means of the thin film hydration method.[34] The latter procedure consists of two key-steps, namely a first step that leads to the lipidic film that is hydratated (second step) with a saline buffer solution (HEPES/NaCl mole ratio 1/6.75). Vesicles were formulated by using 72% (for LP1) or 87% (for LP2) of POPC (1-palmitoyl-2-oleoyl-*sn*-glycero-3-phosphocholine), 10% of cholesterol and 3% of DSPE-PEG-methoxy-2000 (1,2-distearoyl-*sn*-glycero-3-phosphoethanolamine-*N*-[methoxy (polyethyleneglycol)-2000] (ammonium salt)). For LP1, 15% of **1** was mixed with the lipidic components to yield the lipidic film. In LP2, **1** was dissolved in the hydration solution (20 mM). By the latter procedure, DPA-C_6-(Gd)DOTAMA is encapsulated in the aqueous cavity of the liposome. The mean hydrodynamic diameters of the liposomes were determined by dynamic light scattering. They were found to be very similar thus showing that the methodology of preparation is not as relevant as the formulation in determining the final size of the vesicles (Table 3).

Table 2. Best fitting parameters for DPA-C_6-(Gd)DOTAMA/HSA

	Δ^2 ($10^{19}\,s^{-2}$)	τ_v (ps)	τ_r (ps)	τ_m (μs)	q
DPA-C_6-(Gd)DOTAMA/HSA	1.15	24	59 000	1.1	1

The relaxivity values, measured at 25 °C at 20 MHz, were found to be 9.69 and 7.85 $mM^{-1}\,s^{-1}$ for LP1 and LP2, respectively. These values are higher than the value obtained for free **1**, as consequence of the interaction with the liposome membrane. Overall, the observed relaxation enhancement is lower than the one usually observed for amphiphilic Gd complexes interacting with a liposomial membrane. For both types of liposomes, one may think that an equilibrium is occurring in the inner cavity for which DPA-C_6-(Gd)DOTAMA distributes between the inner membrane layer and the aqueous solution. Thus, the NMRD profiles of both liposomes were analyzed taking into account either the contribution due to **1** 'free' (in the inner cavity) and the one due to **1** incorporated in the membrane. Equation (1) has been used:

$$r_{1p} = X^{free} \cdot r_{1p}{}^{free} + X^{bound} \cdot r_{1p}{}^{bound} \quad (1)$$

where X^{bound} and X^{free} are the molar fraction of **1** that is bound or not bound to the liposome's membrane, $r_{1p}{}^{free}$ is the relaxivity value of **1** (6.02 $mM^{-1}\,s^{-1}$) and $r_{1p}{}^{bound}$ is the relaxivity value of the adduct DPA-C_6-(Gd)DOTAMA-liposome. We fixed the latter value to 16 $mM^{-1}\,s^{-1}$, that is the relaxivity value for analogous Gd-DOTAMA system incorporated in liposome's membrane previously investigated in our laboratory.[35] $1/T_1$ NMRD profiles for both liposome suspensions were acquired in the high field region, namely from 20 to 70 MHz, as it is known that for paramagnetic macromolecular systems, this is the field strength where the acquired T_1 data are less prone to yield erroneous results in the fitting procedure. On the basis of X^{free} and X^{bound} values (obtained from K_A) the NMRD profiles of the $r_{1p}{}^{bound}$

Table 3. Liposome formulations and main parameters

	Membrane	Molar ratio	Cavity	Dimension (nm)	r_{1p} ($mM^{-1}\,s^{-1}$)[a]
LP1	POPC	72%	Saline buffer	151	9.69
	Chol	10%			
	DSPE-PEG-metoxy 2000	3%			
	DPA-C_6-(Gd)DOTAMA	15%			
LP2	POPC	87%	DPA-C_6-(Gd)DOTAMA 20 mM	149	7.85
	Chol	10%			
	DSPE-PEG-metoxy 2000	3%			

[a]Measured at 25 °C at 20 MHz.

values for the two types of liposomes have been extracted (Figure 3).

The calculated NMRD profiles of the bound fraction were then fitted as earlier recalled,[32] and the best fitting values for the relevant parameters are reported in Table 4.

The 'humps' at high magnetic field observed for both liposomes are an indication that part of the Gd complex is interacting with the liposomial membrane. As discussed earlier, the detection of a relaxivity enhancement at 30–40 MHz is an indication of the occurrence of an increased τ_r with respect to the value found for the free complex. Also, the exchange lifetime of the coordinated water molecule (τ_m) appears slightly increased upon entrapment of the Gd complex in the liposome. This behavior may be accounted for in terms of a slight distortion in the co-ordination cage geometry upon the binding of the lipophilic moiety to the liposome's membrane.

The relaxivity of DPA-C_6-(Gd)DOTAMA (**1**) loaded liposomes was then measured in the presence of increasing amounts of albumin (HSA) to evaluate whether some amount of **1** could transfer from the liposome to HSA. The Gd-loaded liposomes were challenged with increasing concentrations of albumin (from 0.1 to 0.8 mM), but the relaxation rate (R_{1oss}) values remained unchanged. Although the relaxivity of **1** bound to HSA is similar to that of **1** incorporated in the liposome's membrane, one would expect that the release of **1** from liposomes to HSA causes an overall shift of concentration of **1** either in the aqueous cavity or in the phospholipide bilayer. Such a shift would be related to the amount of added HSA, and it would result in a change of the observed water proton relaxation rate. The observed constancy of R_1 clearly indicates that the Gd-complex is not leaving the liposomes in the presence of HSA in the suspending medium. This result is encouraging in the light of future *in vivo* experiments as DPA-C_6-(Gd)DOTAMA loaded liposomes appear to be a stable carrier for improving the blood lifetime of this imaging agent.

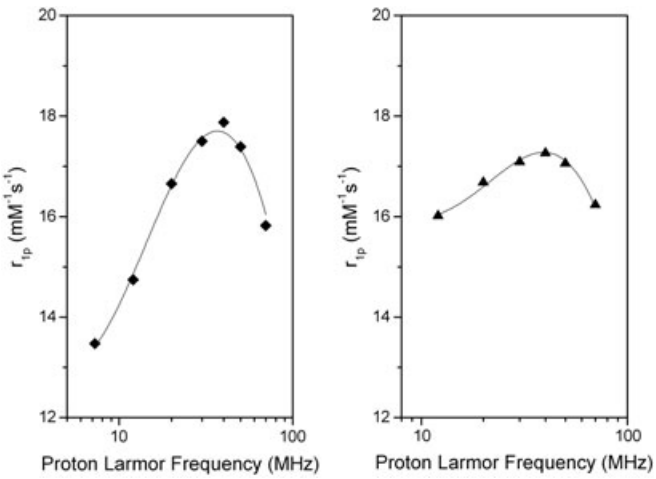

Figure 3. $1/T_1$ nuclear magnetic resonance dispersion profile of 1 mM aqueous solution of LP1 (♦) and LP2 (▲) at 25 °C and pH = 7.4.

Table 4. Best fitting parameters for liposomes LP1 and LP2

	Δ^2 (10^{19} s^{-2})	τ_v (ps)	τ_r (ps)	τ_m (μs)	q
LP1	1.56	0.15	3000	0.88	1
LP2	1.19	7.06	2500	0.87	1

Conclusion

The 2-phenylpyrazolo[1,5-a]pyrimidineacetamide DPA-713 was successfully derivatized and coupled to the DOTA cage. The resulting ligand was complexed with gadolinium. The relaxivity of the obtained Gd-complex was slightly higher (6.02 mM^{-1} s^{-1} at 20 MHz) than the previously reported ones for analogous Gd-DOTAMA complexes, which is in accordance with its increased molecular weight. The NMRD profile is consistent with the one expected for a small, fast tumbling gadolinium complex. Interaction with HSA was assessed and a K_A of 1100 M^{-1} was calculated. Incorporation into liposomes displayed a relaxivity 'hump' in the NMRD profile, as a demonstration of the formation of a supramolecular adduct. Interestingly, it has been found that the amphiphilic DPA-C_6-(Gd)DOTAMA complex can be either incorporated in the liposomial membrane and in the inner aqueous cavity. Overall, the availability of liposomes loaded with this complex is promising for future *in vivo* studies with increased half-life in blood stream and encourages pursuing the task of the slow release of MRI targeting agents.

Experimental Section

1-palmitoyl-2-oleoyl-*sn*-glycero-3-phosphocholine (POPC) and 1,2-distearoyl-*sn*-glycero-3-phosphoethanolamine-*N*-[methoxy(polyethylene glycol)-2000] (ammonium salt) (DSPE-PEG-methoxy-2000) were purchased from Avanti Polar Inc. (Alabaster, Al, USA); DOTA(tBu)$_3$ was purchased from CheMatech, and all the other chemicals were purchased from Sigma-Aldrich and used with no further purification. Solvents were stored over molecular sieves and purged with argon before use. Column chromatographies were conducted on silica gel (0.63–0.200 mm, VWR). Thin layer chromatography (TLC) was carried out using aluminum pre-coated plates of silica gel 60 F_{254} (VWR). Compounds were detected using a UV-lamp (254 nm) and by sprinkling the TLC plate with $KMnO_4$ aqueous solution or ninhydrin/ethanol solution and heating.

^{1}H-NMR and ^{13}C-NMR spectra for characterization of synthesized products were recorded on a Bruker (Wissembourg, France) Avance (400 MHz) apparatus or on a Bruker Avance600 apparatus using the hydrogenated residue of the deuterated solvents $CDCl_3$ (δ = 7.26 ppm), CD_2Cl_2 (δ = 5.32 ppm) or CD_3OD (δ = 3.31 ppm) for ^{1}H-NMR as well as the deuterated solvents $CDCl_3$ (δ = 77.2 ppm), CD_2Cl_2 (δ = 54.0 ppm) or CD_3OD (δ = 49.0 ppm) as an internal standard for ^{13}C-NMR. Chemical shifts are reported in parts per million (ppm) downfield from TMS. Multiplicities are reported as s (singlet), d (doublet), t (triplet), q (quadruplet), m (multiplet) and b (broad). The mass spectra (MS) were recorded on a Thermo Electron Ion Trap LCQ Deca XP + spectrometer (positive electrospray ionization (ESI+)) or on a Waters 3100 Single quadrupole mass detector.

The longitudinal water proton relaxation rate was measured by using a Stelar Spinmaster (Stelar, Mede, Pavia, Italy) spectrometer operating at 20 MHz by means of the standard inversion recovery sequence. The temperature was controlled with a Stelar VTC-91 air-flow heater equipped with a copper constantan thermocouple (uncertainty of 0.1 °C). The proton $1/T_1$ NMRD profiles were measured over a continuum of magnetic field strength from 0.00024 to 0.47 T (corresponding to 0.0120 MHz proton Larmor frequency) on a Stelar field-cycling relaxometer. The relaxometer works under complete computer control with an absolute

uncertainty in $1/T_1$ of ± 1%. Data points from 0.47 T (20 MHz) to 1.7 T (70 MHz) were collected on a Stelar Spinmaster spectrometer working at variable field.

Liposomes extrusion was carried out with Lipex extruder, Northern Lipids Inc., Canada and the liposomes size measurements were performed on Zetasizer NanoZS Dynamic Light Scattering (Malvern, UK).

Chemistry

N,N-diethyl-2-(2-(4-methoxyphenyl)-5,7-dimethylpyrazolo[1,5-a] pyrimidin-3-yl)acetamide (DPA-713). Synthesized according to Ref. 17.

R_f (CH_2Cl_2/CH_3OH 95/5 v/v): 0.39. ^{1}H-NMR (CD_2Cl_2, 400 MHz) δ 7.75 (2H, d, J = 8.8 Hz, Ar), 6.99 (2H, d, J = 8.8 Hz, Ar), 6.54 (1H, s, Ar), 3.88 (2H, s, CH_2CO), 3.85 (3H, s, OCH_3), 3.51 (2H, q, J = 7.2 Hz, NCH_2CH_3), 3.39 (2H, q, J = 7.2 Hz, NCH_2CH_3), 2.72 (3H, s, $ArCH_3$), 2.53 (3H, s, $ArCH_3$), 1.22 (3H, t, J = 7.2 Hz, NCH_2CH_3), 1.11 (3H, t, J = 7.2 Hz, NCH_2CH_3). ^{13}C-NMR (CD_2Cl_2 100 MHz) δ 170.3 [C, CO], 160.4 [C, Ar], 158.1 [C, Ar], 155.0 [C, Ar], 148.3 [C, Ar], 145.3 [C, Ar], 130.2 [2 × CH, Ar], 127.0 [C, Ar], 114.4 [2 × CH, Ar], 108.7 [CH, Ar], 101.3 [C, Ar], 55.8 [CH_3, OCH_3], 42.8 [CH_2, NCH_2CH_3], 41.0 [CH_2, NCH_2CH_3], 28.6 [CH_2, $COCH_2$], 24.9 [CH_3, $ArCH_3$], 17.1 [CH_3, $ArCH_3$], 14.7 [CH_3, NCH_2CH_3], 13.4 [CH_3, NCH_2CH_3]. MS ESI + (m/z) 367 $[M+H]^+$.

*N,N-diethyl-2-(2-(4-hydroxyphenyl)-5,7-dimethylpyrazolo[1,5-a] pyrimidin-3-yl)acetamide,(DPA-OH, **2**).* Synthesized according to Ref 20.

R_f (CH_2Cl_2/CH_3OH 92/8 v/v): 0.41. ^{1}H-NMR (CD_2Cl_2, 400 MHz) δ 7.56 (2H, d, J = 8.4 Hz, Ar), 6.82 (2H, d, J = 8.4 Hz, Ar), 6.55 (1H, s, Ar), 3.90 (2H, s, CH_2CO), 3.47 (2H, q, J = 7.2 Hz, NCH_2CH_3), 3.37 (2H, q, J = 7.2 Hz, NCH_2CH_3), 2.71 (3H, s, $ArCH_3$), 2.52 (3H, s, $ArCH_3$), 2.21 (1H, bs, OH), 1.18 (3H, t, J = 7.2 Hz, NCH_2CH_3), 1.09 (3H, t, J = 7.2 Hz, NCH_2CH_3). ^{13}C-NMR (CD_2Cl_2 100 MHz) δ 171.2 [C, CO], 158.7 [C, Ar], 158.2 [C, Ar], 155.8 [C, Ar], 148.2 [C, Ar], 145.8[C, Ar], 130.4 [2 × CH, Ar], 125.4 [C, Ar], 116.0 [2 × CH, Ar], 108.9 [CH, Ar], 100.8 [C, Ar], 43.0 [CH_2, NCH_2CH_3], 41.4 [CH_2, NCH_2CH_3], 28.7 [CH_2, $COCH_2$], 24.7 [CH_3, $ArCH_3$], 17.2 [CH_3, $ArCH_3$], 14.4 [CH_3, NCH_2CH_3], 13.3 [CH_3, NCH_2CH_3]. MS ESI + (m/z) 353. $M+H]^+$.

*tert-Butyl (6-(4-(3-(2-(diethylamino)-2-oxoethyl)-5,7-dimethylpyrazolo [1,5-a]pyrimidin-2-yl)phenoxy)hexyl)carbamate (**3**). Step 1. 6-((tert-butoxycarbonyl)amino)hexyl 4-methylbenzenesulfonate) synthesis.* Under argon atmosphere, 6-(Boc-amino)1-hexanol (1 g, 4.6 mmol) was dissolved in 25 ml of dichloromethane. Triethylamine (1.28 ml, 9.2 mmol), para-toluenesulfonyl chloride (1.05 g, 5.52 mmol) and a catalytic amount of DMAP were added. The solution was stirred at room temperature overnight. After this time, the solvent was evaporated, and the residue was partitioned between ethyl acetate (150 ml) and HCl 0.1 M aqueous solution (150 ml). The organic layer was separated, and the aqueous phase was extracted with EtOAc (2 × 150 ml); the combined organic layers were washed once with brine (150 ml), dried over Na_2SO_4, filtered and concentrated under reduced pressure. The crude was purified on silica gel (heptane/acetone 80/20) to afford 6-((*tert*-butoxycarbonyl)amino)hexyl 4-methylbenzenesulfonate (1.47 g, 83%) as a colorless oil. R_f (heptane/EtOAc 1/1 v/v): 0.50. ^{1}H-NMR ($CDCl_3$, 400 MHz) δ 7.77 (2H, d, J = 8.0 Hz, Ph), 7.34 (2H, d, J = 8 Hz, Ph), 4.00 (2H, t, J = 6.4 Hz $TsOCH_2$), 3.05 (2H, m, CH_2CH_2NHBoc), 2.44 (3H, s, $PhCH_3$), 1.63 (2H, m, $TsOCH_2CH_2$), 1.42 (9H, s, *t*-Bu), 1.39–1.24 (6H, m, 3 × CH_2). ^{13}C-NMR ($CDCl_3$ 100 MHz) δ 156.1 [C, CO], 144.8 [C, Ph], 133.3 [C, Ph], 130 [2 × CH, Ph], 128.0 [2 × CH, Ph], 79.2 [C, $C(CH_3)_3$], 70.6 [CH_2, $TsOCH_2$], 40.5 [CH_2, CH_2NHBoc], 30.0 [CH_2], 28.8 [CH_2], 28.5 [3 × CH_3, *t*-Bu], 26.2 [CH_2], 25.2 [CH_2], 21.7 [CH_3, $PhCH_3$].

Step 2. DPA-OH (**2**) (1.17 g, 3.33 mmol) was dissolved in 50 ml of DMSO, then NaOH (0.23 g, 6.66 mmol) and 6-((*tert*-butoxycarbonyl)amino)hexyl 4-methylbenzenesulfonate (1.47 g, 4.00 mmol) were added. The solution was stirred at 50 °C overnight. The reaction was poured onto a saturated aqueous solution of K_2CO_3 (150 ml) and extracted twice with EtOAc (2 × 200 ml). The combined organic layers were washed twice (2 × 200 ml) with brine, dried over Na_2SO_4, filtered and concentrated under reduced pressure. The crude was purified on silica gel using CH_2Cl_2/CH_3OH 98/2 v/v as eluent to afford the desired product **3** (1.07 g, 61%) as a yellow solid. R_f (CH_2Cl_2/CH_3OH 95/5 v/v): 0.33. ^{1}H-NMR ($CDCl_3$, 400 MHz) δ 7.75 (2H, d, J = 8.8 Hz, Ar), 6.96 (2H, d, J = 8.8 Hz, Ar), 6.50 (1H, s, Ar), 3.99 (2H, t, J = 6.4 Hz, $ArOCH_2$), 3.91 (2H, s, $CH_2C=O$), 3.50 (2H, q, J = 7.2 Hz, NCH_2CH_3), 3.41 (2H, q, J = 7.2 Hz, NCH_2CH_3), 3.13 (2H, m, CH_2NHBoc), 2.73 (3H, s, $ArCH_3$), 2.53 (3H, s, $ArCH_3$), 1.80 (2H, m, OCH_2CH_2), 1.53–1.39 (6H, m, 3 × CH_2), 1.44 (9H, s, *t*-Bu), 1.20 (3H, t, J = 7.2 Hz, NCH_2CH_3), 1.11 (3H, t, J = 7.2 Hz, NCH_2CH_3). ^{13}C-NMR ($CDCl_3$, 100 MHz) δ 170.2 [C, C=O], 159.1 [C, Ar], 157.6 [C, Ar], 156.2 [C, C=O], 155.2 [C, Ar], 147.8 [C, Ar], 144.8 [C, Ar], 130.0 [2 × CH, Ar], 126.3 [C, Ar], 114.6 [2 × CH, Ar], 108.2 [CH, Ar], 100.9 [C, Ar], 79.2 [C, $C(CH_3)_3$], 67.9 [CH_2, $ArOCH_2$], 42.4 [CH_2, NCH_2CH_3], 40.7 [CH_2, NCH_2CH_3], 30.2 [CH_2, CH_2NHBoc], 29.3 [CH_2], 28.5 [3 × CH_3, *t*-Bu], 28.3 [CH_2], 26.7 [CH_2], 25.9 [2 × CH_2], 24.8 [CH_3, $ArCH_3$], 17.1 [CH_3, $ArCH_3$], 14.5 [CH_3, NCH_2CH_3], 13.2 [CH_3, NCH_2CH_3]. MS ESI + (m/z) 553 $[M+H]^+$, 574 $[M+Na]^+$.

*2-(2-(4-((6-aminohexyl)oxy)phenyl)-5,7-dimethylpyrazolo[1,5-a]pyrimidin-3-yl)-N,N-diethylacetamide (**4**).* Compound **3** (1.80 g, 3.26 mmol) was dissolved in 50 ml of dichloromethane and trifluoroacetic acid (10 ml, 132 mmol) was added. The solution was stirred at room temperature overnight. The reaction was then evaporated to dryness, and the residue was partitioned between a saturated aqueous solution of K_2CO_3 and EtOAc. The organic layer was collected, and the aqueous phase was washed twice with EtOAc. The resulting organic layers were combined to the first one. The combined organic layers were washed with brine, dried over Na_2SO_4, filtered and concentrated under reduced pressure. The crude was purified on silica gel (CH_2Cl_2/CH_3OH 90/10) to afford the desired product (1.47 g, 80%) as an oil. R_f (CH_2Cl_2/CH_3OH 80/20 v/v): 0.25. ^{1}H-NMR (CD_3OD, 400 MHz) δ 7.62 (2H, d, J = 8.4 Hz, Ar), 7.13 (1H, s, Ar), 7.06 (2H, d, J = 8.4 Hz, Ar), 4.07 (4H, m, $ArOCH_2$, CH_2CO), 3.56 (2H, q, J = 7.2 Hz, NCH_2CH_3), 3.44 (2H, q, J = 7.2 Hz, NCH_2CH_3), 2.95 (5H, m, CH_2NH_2 + $ArCH_3$), 2.77 (3H, s, $ArCH_3$), 1.86 (2H, m, OCH_2CH_2), 1.71 (2H, m, CH_2NH_2), 1.60–1.50 (4H, m, 2 × CH_2), 1.27 (3H, t, J = 7.2 Hz, NCH_2CH_3) 1.16 (3H, t, J = 7.2 Hz, NCH_2CH_3). ^{13}C-NMR (CD_3OD, 100 MHz) δ 171.0 [C, C=O], 161.9 [C, Ar], 159.8 [C, Ar], 159.0 [C, Ar], 155.5 [C, Ar], 141.5 [C, Ar], 131.2 [2 × CH, Ar], 125.0 [C, Ar], 115.9 [2 × CH, Ar], 109.3 [CH, Ar], 100.0 [C, Ar], 69.0 [CH_2, $ArOCH_2$], 43.8 [CH_2, NCH_2CH_3], 42.2 [CH_2, NCH_2CH_3], 40.7 [CH_2, CH_2NH_2], 30.1 [CH_2], 28.8 [CH_2], 28.5 [CH_2], 27.2 [CH_2], 26.7 [CH_2], 21.1 [CH_3, $ArCH_3$], 17.9 [CH_3, $ArCH_3$], 14.3 [CH_3, NCH_2CH_3], 13.3 [CH_3, NCH_2CH_3]. MS ESI + (m/z) 452 $[M+H]^+$.

*2,2′,2″-(10-(2-((6-(4-(3-(2-(diethylamino)-2-oxoethyl)-5,7-dimethylpyrazolo[1,5-a]pyrimidin-2-yl)phenoxy)hexyl)amino)-2-oxoethyl)-1,4,7,10-tetraazacyclododecane-1,4,7-triyl)triacetic acid (**5**)[30].* $DOTA(tBu)_3$ (0,500 g, 0.87 mmol) was dissolved in 25 ml of DMF. TBTU (0,28 g, 0.87 mmol), DIPEA (1.72 ml, 6.70 mmol) and compound **4** (0,327 g, 0,67 mmol) were added. The solution was stirred at

room temperature for 24 h. The reaction was partitioned between water and EtOAc. The aqueous phase was acidified to pH 5–6, and extracted twice with EtOAc. The collected organic layers were washed once with water and once with brine, dried over Na_2SO_4, filtered and evaporated under reduced pressure. The residue was purified on silica gel using CH_2Cl_2/CH_3OH 95/5 v/v as eluent, yielding the desired product **5** as a yellow solid (0.55 g, 80%). R_f (CH_2Cl_2/CH_3OH 90/10 v/v): 0.22. ^{1}H-NMR (CD_3OD, 400 MHz) δ 7.64 (2H, d, J = 8.8 Hz, Ar), 7.00 (2H, d, J = 8.8 Hz, Ar), 6.79 (1H, s, Ar), 4.03 (2H, t, J = 6.0 Hz, $ArOCH_2$), 3.96 (2H, s, $CH_2C=O$), 3.60–2.50 (8H, b, 4 × $NCH_2COOtBu$), 3.56 (2H, q, J = 7.2 Hz, NCH_2CH_3), 3.41 (2H, q, J = 7.2 Hz, NCH_2CH_3), 3.22 (2H, t, J = 6.8 Hz, CH_2NH-DOTA(tBu)$_3$), 2.75 (3H, s, $ArCH_3$), 2.56 (3H, s, $ArCH_3$), 2.50–2.00 (16H, b, 8 × CH_2) 1.81 (2H, m, OCH_2CH_2), 1.60–1.30 (6H, m, 3 × CH_2), 1.49 (27H, s, 3 × *t*-Bu), 1.24 (3H, t, J = 7.2 Hz, NCH_2CH_3), 1.12 (3H, t, J = 7.2 Hz, NCH_2CH_3). ^{13}C-NMR (CD_3OD, 100 MHz) δ 174.4 [2 × C, C=O], 174.1 [C, C=O], 173.1 [C, C=O], 172.3 [C, C=O], 161.1 [C, Ar], 160.0 [C, Ar], 156.5 [C, Ar], 148.9 [C, Ar], 147.0 [C, Ar], 131.0 [2 × CH, Ar], 126.9 [C, Ar], 115.5 [2 × CH, Ar], 109.7 [CH, Ar], 101.5 [C, Ar], 82.8 [3 × C, $C(CH_3)_3$], 68.9 [CH_2, $ArOCH_2$], 57.2 [CH_2, NCH_2CON], 56.8 [CH_2, $NCH_2COOtBu$], 56.7 [2 × CH_2, $NCH_2COOtBu$], 55–51 [8 × CH_2, b, CH_2], 43.6 [CH_2, NCH_2CH_3], 42.0 [CH_2, NCH_2CH_3], 40.2 [CH_2], 30.8 [CH_2], 30.3 [CH_2], 28.9 [CH_2], 28.5 [9 × CH_3, 3 × *t*-Bu], 27.8 [CH_2], 27.0 [CH_2], 24.2 [CH_3, $ArCH_3$], 16.9 [CH_3, $ArCH_3$], 14.3 [CH_3, NCH_2CH_3], 13.3 [CH_3, NCH_2CH_3]. MS ESI + (*m/z*) 1028 $[M+Na]^+$.

*2,2′,2″-(10-(2-((6-(4-(3-(2-(diethylamino)-2-oxoethyl)-5,7-dimethylpyrazolo[1,5-a]pyrimidin-2-yl)phenoxy)hexyl)amino)-2-oxoethyl)-1,4,7,10-tetraazacyclododecane-1,4,7-triyl)triacetic acid (**6**).* To a solution of **5** (0.72 g, 0.72 mmol) in dichloromethane (5 ml), neat trifluoroacetic acid (0.22 ml, 2.88 mmol) was slowly added and the solution was stirred at RT for 1 h. The dichloromethane was evaporated and trifluoroacetic acid (0.22 ml, 2.88 mmol) was added to the residue. The solution was stirred for 24 h, then diethyl ether was slowly added (20 ml) to give a yellow-orange solid, which was filtered, washed with diethyl ether and dried. The crude was purified on FPLC (Akta Purifier, Pharmacia) on amberchrom CG161 by using isocratic gradient water/methanol as eluent to afford a yellow solid (0.245 g, 33%). ^{1}H-NMR (CD_3OD, 600 MHz) δ 7.62 (2H, d, J = 8.4 Hz, Ar), 7.00 (2H, d, J = 8.4 Hz, Ar), 6.76 (1H, s, Ar), 4.03 (2H, t, J = 6.6 Hz, $ArOCH_2$), 3.94 (2H, s, $CH_2C=O$), 3.75–3.30 (8H, b, 3 × NCH_2COOH + 1 × NCH_2CONH), 3.54 (2H, m, NCH_2CH_3), 3.40 (2H, m, NCH_2CH_3), 3.21 (2H, t, J = 7.2 Hz, CH_2NH-DOTA), 2.74 (3H, s, $ArCH_3$), 2.56 (3H, s, $ArCH_3$), 3.30–2.00 (16H, b, 8 × CH_2), 1.81 (2H, m, OCH_2CH_2), 1.60–1.35 (6H, m, 3 × CH_2), 1.24 (3H, t, J = 7.2 Hz, NCH_2CH_3), 1.12 (3H, t, J = 7.2 Hz, NCH_2CH_3).^{13}C-NMR (CD_3OD, 150 MHz) δ 174.7 [2 × C, CON], 172.3 [C, COOH], 171.8 [C, COOH], 170.0 [C, COOH], 161.1 [C, Ar], 160.0 [C, Ar], 156.5 [C, Ar], 148.8 [C, Ar], 146.9 [C, Ar], 130.9 [2 × CH, Ar], 126.8 [C, Ar], 115.6 [2 × CH, Ar], 109.7 [CH, Ar], 101.5 [C, Ar], 69.0 [CH_2, OCH_2], 57.6 [CH_2, NCH_2CON], 56.7 [CH_2, $NCH_2COOtBu$], 54.9 [2 × CH_2, $NCH_2COOtBu$], 52.3–49.5 [8 × CH_2, b, CH_2], 43.6 [CH_2, NCH_2CH_3], 42.0 [CH_2, NCH_2CH_3], 40.5 [CH_2], 30.4 [CH_2], 30.3 [CH_2], 28.9 [CH_2], 27.8 [CH_2], 26.9 [CH_2], 24.2 [CH_3, $ArCH_3$], 16.9 [CH_3, $ArCH_3$], 14.3 [CH_3, NCH_2CH_3], 13.3 [CH_3, NCH_2CH_3]. MS ESI + (*m/z*) 838 $[M+H]^+$, 420 $[(M+2H)/2]^+$, 280 $[(M+3H)/3]^+$.

*Gadolinium(III) 2,2′,2″-(10-(2-(6-(4-(3-(2-(diethylamino)-2-oxoethyl)-5,7-dimethylpyrazolo[1,5-a]pyrimidin-2-yl)phenoxy)hexylamino)-2-oxoethyl)-1,4,7,10-tetraazacyclododecane-1,4,7-triyl)triacetate (**1**).*
The complexation of **6** was performed with $GdCl_3$ in aqueous solution at pH 6.5 by the method of addition of the ligand.[31] An equimolar amount of $GdCl_3 \times 6H_2O$ (45 mg, 0.12 mmol) solution in water was added to the aqueous solution of ligand **6** (102 mg, 0.12 mmol), maintaining the pH value at 6.5 with NaOH 0.1 N. The mixture was allowed to stir at RT until the pH remained constant at 6.5. The solution was then lyophilized to give a pale yellow solid (150 mg, impurities are only salts). The amount of residual free Gd^{3+} ion was assessed by the orange xylenol UV method,[36] and the corresponding amount of ligand was added to avoid the presence of free Gd ions. MS ESI + (*m/z*) 992 $[M+H]^+$, 496 $[(M+2H)/2]^+$.

Liposomes preparation, general procedure

Large unilamellar vescicles (LUV) were prepared following the thin film hydration method.[34] Briefly, the lipids were dissolved in chloroform or chloroform/methanol solution, and the organic solution was slowly evaporated until the thin film was formed. The film was then hydrated at 55 °C with 1.45 ml of saline buffer (HEPES/NaCl mole ratio 1/6.75) to obtain a total lipid amount of 30 mg/ml. The resulting suspension of multilamellar vescicles was extruded three times through polycarbonate filters of 400 nm and five times through 200 nm filters. The final suspension was then purified by exhaustive dialysis carried out at 4 °C in saline buffer. The liposomes were characterized by dynamic light scattering (Zetasizer NanoZS, Malvern, UK) in order to assess the mean hydrodynamic size and the polydispersity of the system.

LP1: 72% POPC, 10% cholesterol, 3% DSPE-PEG-methoxy 2000, 15% DPA-C_6-(Gd)DOTAMA were dissolved in 10 ml of chloroform/methanol solution (7/3 v/v). The formed thin film was hydratated with saline buffer and then was extruded. The mean hydrodynamic diameter was 151 nm with a polydispersity index (PDI) of 0.07.

LP2: 87% POPC, 10% cholesterol and 3% DSPE-PEG-methoxy 2000 were dissolved in 10 ml of chloroform. The thin film was hydratated with saline buffer containig DPA-C_6-(Gd)DOTAMA 20 mM. The mean hydrodynamic diameter was 149 nm with a PDI of 0.10

Acknowledgements

This work was supported in part by intramural programs, as well as the FP6 European Networks of Excellence EMIL (Grant LSHC-CT-2004-503569) and DiMI (Grant LSHB-CT-2005-512146), and more recently the European Union's Seventh Framework Programme [FP7/2007-2013] INMiND (Grant agreement no. HEALTH-F2-2011-278850). Part of the present work was also carried out in the frame of COST TD1004 Action ('Theranostics'). The authors also wish to thank Dr Dirk Roeda for proofreading the manuscript and suggesting linguistic corrections.

References

[1] V. Papadopoulos, M. Baraldi, T. B. Guilarte, T. B. Knudsen, J. J. Lacapère, P. Lindemann, M. D. Norenberg, D. Nutt, A. Weizman, M. R. Zhang, M. Gavish. *Trends Pharmacol. Sci.* **2006**, *27*, 402–409.
[2] R. Rupprecht, V. Papadopoulos, G. Rammes, T. C. Baghai, J. Fan, N. Akula, G. Groyer, D. Adams, M. Schumacher. *Nat. Rev. Drug Discov.* **2010**, *9*, 971–988.
[3] V. Papadopoulos, J. Liu, M. Culty. *Mol. Cell. Endocrinol.* **2007**, *266*, 59–67.
[4] P. Casellas, S. Galiegue, A. S. Basile. *Neurochem. Int.* **2002**, *40*, 475–486.
[5] M. Gavish, I. Bachman, R. Shoukrun, Y. Katz, L. Veenman, G. Weisinger, A. Weizman. *Pharmacol. Rev.* **1999**, *51*, 629–650.
[6] R. R. Anholt, K. M. Murphy, G. E. Mack, S. H. Snyder. *J. Neurosci.* **1984**, *4*, 593–603.
[7] G. T. Bolger, E. Mezey, J. Cott, B. A. Weissman, S. M. Paul, P. Skolnick. *Eur. J. Pharmacol.* **1984**, *105*, 143–148.
[8] D. Decaudin, M. Castedo, F. Nemati, A. Beurdeley-Thomas, G. De Pinieux, A. Caron, P. Pouillart, J. Wijdenes, D. Rouillard, G. Kroemer, M. F. Poupon. *Cancer Res.* **2002**, *62*, 1388–1393.

[9] L. A. Karchewski, S. Bloechlinger, C. J. Woolf. *Eur. J. Neurosci.* **2004**, *20*, 671–683.
[10] S. Galiegue, N. Tinel, P. Casellas. *Curr. Med. Chem.* **2003**, *10*, 1563–1572.
[11] R. B. Banati. *Glia* **2002**, *40*, 206–217.
[12] F. Chauveau, H. Boutin, N. Van Camp, F. Dollé, B. Tavitian. *Eur. J. Nucl. Med. Mol. Imaging* **2008**, *35*, 2304–2319.
[13] F. Dollé, C. Luus, A. Reynolds, M. Kassiou. *Curr. Med. Chem.* **2009**, *16*, 2899–2923.
[14] D. Roeda, B. Kuhnast, A. Damont, F. Dollé. *J. Fluorine Chem.* **2012**, *134*, 107–114.
[15] S. Selleri, F. Bruni, C. Costagli, A. Costanzo, G. Guerrini, G. Ciciani, B. Costa, C. Martini. *Bioorg. Med. Chem.* **2001**, *9*, 2661–2671.
[16] S. Selleri, P. Gratteri, C. Costagli, C. Bonaccini, A. Costanzo, F. Melani, G. Guerrini, G. Ciciani, B. Costa, F. Spinetti, C. Martini, F. Bruni. *Bioorg. Med. Chem.* **2005**, *13*, 4821–4834.
[17] M. L. James, R. R. Fulton, D. J. Henderson, S. Eberl, S. R. Meikle, S. Thomson, R. D. Allan, F. Dollé, M. J. Fulham, M. Kassiou. *Bioorg. Med. Chem.* **2005**, *13*, 6188–6194.
[18] C. Thominiaux, F. Dollé, M. L. James, Y. Bramoullé, H. Boutin, L. Besret, M. C. Grégoire, H. Valette, M. Bottlaender, B. Tavitian, P. Hantraye, S. Selleri, M. Kassiou. *Appl. Radiat. Isot.* **2006**, *64*, 570–573.
[19] H. Boutin, F. Chauveau, C. Thominiaux, B. Kuhnast, M. C. Grégoire, M. L. James, S. Jan, V. Brulon, Y. Fontyn, S. Selleri, R. Trébossen, P. Hantraye, F. Dollé, B. Tavitian, M. Kassiou. *J. Nucl. Med.* **2007**, *48*, 573–581.
[20] A. Damont, F. Hinnen, B. Kuhnast, M. A. Schollhorn-Peyronneau, M. James, C. Luus, B. Tavitian, M. Kassiou, F. Dollé. *J. Labelled Compd. Radiopharm.* **2008**, *51*, 286–292.
[21] M. L. James, R. R. Fulton, J. Vercoullie, D. J. Henderson, L. Garreau, S. Chalon, F. Dollé, S. Selleri, D. Guilloteau, M. Kassiou. *J. Nucl. Med.* **2008**, *49*, 814–822.
[22] F. Chauveau, N. Van Camp, F. Dollé, B. Kuhnast, C. Thominiaux, F. Hinnen, A. Damont, H. Boutin, M. L. James, M. Kassiou. *J. Nucl. Med.* **2009**, *50*, 468–476.
[23] A. Martín, R. Boisgard, B. Thézé, N. Van Camp, B. Kuhnast, A. Damont, M. Kassiou, F. Dollé, B. Tavitian. *J. Cereb. Blood Flow Metab.* **2010**, *30*, 230–241.
[24] A. Martin, R. Boisgard, M. Kassiou, R. Dollé, B. Tavitian. *Mol. Imaging Biol.* **2011**, *13*, 10–15.
[25] J. Zheng, R. Boisgard, K. Siquier-Pernet, D. Decaudin, F. Dollé, B. Tavitian. *Mol. Pharm.* **2011**, *8*, 823–832.
[26] G. Abourbeh, B. Thézé, R. Maroy, A. Dubois, V. Brulon, Y. Fontyn, F. Dollé, B. Tavitian, R. Boisgard. *J. Neurosci.* **2012**, *32*, 5728–5736.
[27] A. Winkeler, R. Boisgard, A. R. Awde, A. Dubois, B. Thézé, J. Zheng, L. Ciobanu, F. Dollé, T. Viel, A. H. Jacobs, B. Tavitian. *Eur. J. Nucl. Med. Mol. Imaging* **2012**, *39*, 811–823.
[28] E. Terreno, D. Delli Castelli, A. Viale, S. Aime. *Chem. Rev.* **2010**, *110*, 3019–3042.
[29] A. Reynolds, R. Hanani, D. Hibbs, A. Damont, E. Da Pozzo, S. Selleri, F. Dollé, C. Martini, M. Kassiou. *Bioorg. Med. Chem. Lett.* **2010**, *20*, 5799–5802.
[30] M. Halim, M. S. Tremblay, S. Jockusch, N. J. Turro, D. Sames. *J. Am. Chem. Soc.* **2007**, *129*, 7704–7705.
[31] S. Geninatti Crich, C. Cabella, A. Barge, S. Belfiore, S. Colombatto, D. Corpillo, C. Ghirelli, L. Lattuada, S. Lanzardo, A. Mortillaro, L. Tei, M. Visigalli, G. Forni, S. Aime. *J. Med. Chem.* **2006**, *49*, 4926–4936.
[32] S. Aime, M. Botta, E. Terreno. *Adv. Inorg. Chem.* **2005**, *57*, 173–237.
[33] S. Aime, M. Botta, M. Fasano, E. Terreno, in *The Chemistry of Contrast Agents*, (Eds: A. Merbach, E. Toth), John Wiley & Sons, Chichester, UK, **2001**, p. 193.
[34] J. Lasch, V. Weissig, M. Brandl, in *Liposomes. A Pratical Approach*, (Eds: V. P. Torchilin, V. Weissig), Oxford University Press, **2003**, p. 3.
[35] E. Gianolio, S. Porto, R. Napolitano, S. Baroni, G. B. Giovenzana, S. Aime. *Inorg. Chem.* **2012**, *51*, 7210–7217.
[36] A. Barge, G. Cravotto, E. Gianolio, F. Fedeli. *Contrast Med. Mol. Imaging* **2006**, *1*, 184–188.